J|A|C|S ARTICLES

Published on Web 05/11/2009

Collagen Targeting Using Protein-Functionalized Micelles: The Strength of Multiple Weak Interactions

Sanne W. A. Reulen,[†] Patricia Y. W. Dankers,[†,‡] Paul H. H. Bomans,[§] E. W. Meijer,[†] and Maarten Merkx*[,†]

Laboratory of Chemical Biology, Department of Biomedical Engineering, Eindhoven University of Technology, P.O. Box 513, 5600 MB Eindhoven, The Netherlands, Stem Cell and Tissue Engineering Group, Department of Pathology and Medical Biology, University of Groningen, University Medical Center Groningen, Hanzeplein 1, 9713 GZ Groningen, The Netherlands, and Soft Matter CryoTEM Research Unit, Department of Chemical Engineering and Chemistry, Eindhoven University of Technology, P.O. Box 513, 5600 MB Eindhoven, The Netherlands

Received September 30, 2008; E-mail: m.merkx@tue.nl

Abstract: Collagen is an important marker for the assessment of tissue remodeling, both in normal tissue maturation and in a variety of prevalent disease processes. Given the importance of multivalency in the natural interactions of collagen, multivalent ligands provide unique opportunities to target collagen architectures. Here, we explored the use of micelles as dynamic self-assembling multivalent scaffolds for the collagen binding protein CNA35. Despite the increased popularity of micelles as nanosized carriers in targeted drug delivery and molecular imaging, few studies have actually directly addressed the importance of multivalent interactions for micelle-based targeting. Native chemical ligation was used as a chemoselective and efficient method to prepare relatively well-defined and stable micelles with a tunable average protein content between 0 and 20 copies of CNA35 per micelle. The thermodynamics and kinetics of CNA35 micelle binding to collagen was studied using solid-phase and surface plasmon resonance assays. Multivalent interactions between the micelles and collagen had a remarkable effect on micellar stability, since no dissociation of collagen-bound micelles was observed even after extensive washing. In addition, an impressive enhancement of collagen affinity was observed both in vitro and ex vivo resulting from multivalent display of a so-called "nonbinding" variant of CNA35. This "restoration" of collagen affinity was subsequently also observed for liposomes displaying the same low-affinity CNA35 variant at a sufficient density. These results demonstrate the importance of multivalent interactions for micelle-based targeting and illustrate the strength of multiple weak interactions when targeting intrinsically multivalent extracellular matrix (ECM) proteins such as collagen.

Introduction

Micelles have recently gained increased popularity as efficient delivery systems for hydrophobic drugs and as carriers of molecular imaging probes.[1−4] Of special interest are polymeric micelles consisting of pegylated phospholipids, as these combine increased stability, biocompatibility, and high circulation times with a small and well-defined size that allows efficient tissue penetration. Active targeting of micelles to, e.g., tumor tissue[1,5,6] and atherosclerotic plaques,[7] has been reported using a variety of ligands including antibodies,[1,7,8] peptides,[9,10] transferrin,[11] carbohydrates,[12−14] and folic acid.[15] A unique feature of micelles and other nanoparticles is that their size allows them to interact with complex biomolecular architectures using multiple weak interactions simultaneously.[16−18] Self-assembling nanoparticles such as micelles and liposomes present particularly attractive scaffolds for such multivalent ligand display, as their dynamic nature allows reorganization of their structure to best match the architecture of the multivalent target. For liposomes impressive affinity enhancements have been reported, and various aspects of multivalent ligand design have been elucidated, such as the importance of statistical matching between the ligand and receptor density.[19−21] In contrast, few studies have actually experimentally addressed the importance of multivalency for targeting by the more dynamic micelles.

[†] Department of Biomedical Engineering, Eindhoven University of Technology.
[‡] Department of Pathology and Medical Biology, University of Groningen.
[§] Department of Chemical Engineering and Chemistry, Eindhoven University of Technology.

(1) Torchilin, V. P.; Lukyanov, A. N.; Gao, Z.; Papahadjopoulos-Sternberg, B. *Proc. Natl. Acad. Sci. U.S.A.* **2003**, *100*, 6039–6044.
(2) Mulder, W. J.; Strijkers, G. J.; van Tilborg, G. A.; Griffioen, A. W.; Nicolay, K. *NMR Biomed.* **2006**, *19*, 142–164.
(3) Torchilin, V. P. *Pharm. Res.* **2007**, *24*, 1–16.
(4) Mahmud, A.; Xiong, X. B.; Aliabadi, H. M.; Lavasanifar, A. *J. Drug Targeting* **2007**, *15*, 553–584.
(5) Sutton, D.; Nasongkla, N.; Blanco, E.; Gao, J. M. *Pharm. Res.* **2007**, *24*, 1029–1046.
(6) Karmali, P. P.; Kotamraju, V. R.; Kastantin, M.; Black, M.; Missirlis, D.; Tirrell, M.; Ruoslahti, E. *Nanomed.: Nanotechnol., Biol., Med.* **2009**, *5*, 73–82.
(7) Briley-Saebo, K. C.; Shaw, P. X.; Mulder, W. J. M.; Choi, S.-H.; Vucic, E.; Aguinaldo, J. G. S.; Witztum, J. L.; Fuster, V.; Tsimikas, S.; Fayad, Z. A. *Circulation* **2008**, *117*, 3206–3215.
(8) Mulder, W. J. M.; Strijkers, G. J.; Briley-Saboe, K. C.; Frias, J. C.; Aguinaldo, J. G. S.; Vucic, E.; Amirbekian, V.; Tang, C.; Chin, P. T. K.; Nicolay, K.; Fayad, Z. A. *Magn. Reson. Med.* **2007**, *58*, 1164–1170.

10.1021/ja807723p CCC: $40.75

Collagen is an important marker for the assessment of tissue remodeling, both in normal tissue maturation and in a variety of prevalent disease processes.[22−25] For example, collagen is known to be a major indicator for plaque stability in atherosclerosis,[26,27] and Gd-labeled collagen targeting peptides have been employed to visualize scar tissue formation after myocardial infarction using magnetic resonance imaging (MRI).[28,29] Multivalent interactions play an important role in many of the natural interactions of collagens, a classical example being the role of collagen in platelet aggregation.[30,31] The presence of multiple binding sites in close proximity to each other and the hierarchical structural organization of collagens therefore makes them attractive, although complex targets for multivalent interactions.[32,33] CNA35 is a structurally well-characterized 35 kDa collagen binding domain present in an adhesin protein from *Staphylococcus aureus*.[34] CNA35 binds with moderate affinity ($K_d \sim 0.5\ \mu M$) to a variety of different collagen types and was shown to be an excellent fluorescent probe for the visualization of collagen in tissues and life cell cultures.[35−37] Interestingly, display of CNA35 at the exterior of *S. aureus* allows this pathogenic microorganism to interact with exposed collagens present in wounds and was found to play a key role in determining its virulence.[38] Liposomes functionalized with multiple copies of CNA35 were recently found to bind collagen with a low nanomolar affinity.[39] Whether this increase in apparent affinity was due to multivalent binding or a mere statistical effect remained unclear, however.

Here we explored the use of micelles as dynamic, self-assembling multivalent scaffolds for CNA35. We recently reported the synthesis of a cysteine-functionalized pegylated phospholipid (Cys−PEG2000−DSPE) that allows chemoselective conjugation of proteins with a C-terminal thioester using native chemical ligation (NCL).[39] Pegylated phospholipids such as PEG2000−DSPE are known to spontaneously form micelles containing on average 90 lipids per 14 nm micelle and a critical micelle concentration (cmc) of $\sim 5\ \mu M$.[40−42] We reasoned that NCL of CNA35 thioester to Cys−PEG2000−DSPE should result in the formation of relatively stable CNA35 micelles, whose valency could be tuned by simply varying the ratio of protein to Cys−PEG2000−DSPE in the ligation reaction. Binding of these CNA35 micelles to collagen was only observed above a cmc of $\sim 5\ \mu M$, but once bound to collagen the multivalent protein micelles proved to be extremely stable, and no dissociation was observed even after extensive washing. Multivalent display of a "nonbinding" CNA35 mutant was shown to result in full "restoration" of collagen binding affinity, both on micelles and on liposomes, providing an impressive illustration of the potency of multiple weak interactions. These results demonstrate the importance of multivalent interactions for micelle-based targeting and suggest novel means of interrogating the multivalent architecture of collagens.

Experimental Section

Materials. 1,2-Dipalmitoyl-*sn*-glycero-3-phosphoethanolamine-*N*-(lissamine rhodamine B sulfonyl) (rhodamine-DPPE), 1,2-distearoyl-*sn*-glycero-3-phosphocholine (DSPC), 1,2-distearoyl-*sn*-glycero-3-phosphoethanolamine-*N*-[methoxy(poly(ethylene glycol))2000] (PEG−DSPE), and cholesterol were purchased from Avanti Polar Lipids (Albaster, U.S.A). Gd-DTPA-bis(stearylamide) was purchased from Gateway Chemical Technology (St. Louis, MO). Cysteine-functionalized 1,2-distearoyl-*sn*-glycero-3-phosphoethanolamine-*N*-[amino(poly(ethylene glycol))2000] (Cys−PEG−DSPE) was synthesized as described previously.[39] 4-(Carboxylmethyl) thiophenol (MPAA), tris(2-carboxyethyl) phosphine hydrochloride (TCEP), sodium 2-mercaptoethanesulfonate (MESNA), and collagens of rat tail type I (C7661), bovine type II (C1188), human type III (C4407), human type IV (C7521), and human type V (C3657) were purchased from Sigma. Rabbit anticollagen type IV (ab6586) and donkey antirabbit IgG-FITC (ab6798) were purchased from Abcam.

Protein Expression and Purification. The 6His-CNA35 gene was amplified from pQE30CNA35[38] using the primers 5′-GGT GGT CAT ATG AGA GGA TCG CAT CAC C-3′ and 5′-GGT GGT TGC TCT TCC GCA TGC CTT GGT ATC TTT ATC CTG TTT TAA AAC-3′. After digestion with *Nde* I and *Sap* I, the PCR

(9) Nasongkla, N.; Shuai, X.; Ai, H.; Weinberg, B. D.; Pink, J.; Boothman, D. A.; Gao, J. *Angew. Chem., Int. Ed.* **2004**, *43*, 6323–6327.
(10) Xiong, X. B.; Mahmud, A.; Uludag, H.; Lavasanifar, A. *Biomacromolecules* **2007**, *8*, 874–884.
(11) Vinogradov, S.; Batrakova, E.; Li, S.; Kabanov, A. *Bioconjugate Chem.* **1999**, *10*, 851–860.
(12) Jule, E.; Nagasaki, Y.; Kataoka, K. *Langmuir* **2002**, *18*, 10334–10339.
(13) Murthy, B. N.; Voelcker, N. H.; Jayaraman, N. *Glycobiology* **2006**, *16*, 822–832.
(14) Jule, E.; Nagasaki, Y.; Kataoka, K. *Bioconjugate Chem.* **2003**, *14*, 177–186.
(15) Bae, Y.; Jang, W. D.; Nishiyama, N.; Fukushima, S.; Kataoka, K. *Mol. BioSyst.* **2005**, *1*, 242–250.
(16) Mammen, M.; Choi, S. K.; Whitesides, G. M. *Angew. Chem., Int. Ed.* **1998**, *37*, 2755–2794.
(17) Kiessling, L. L.; Gestwicki, J. E.; Strong, L. E. *Curr. Opin. Chem. Biol.* **2000**, *4*, 696–703.
(18) Tu, R. S.; Tirrell, M. *Adv. Drug Delivery Rev.* **2004**, *56*, 1537–1563.
(19) Basha, S.; Rai, P.; Poon, V.; Saraph, A.; Gujraty, K.; Go, M. Y.; Sadacharan, S.; Frost, M.; Mogridge, J.; Kane, R. S. *Proc. Natl. Acad. Sci. U.S.A.* **2006**, *103*, 13509–13513.
(20) Rai, P.; Padala, C.; Poon, V.; Saraph, A.; Basha, S.; Kate, S.; Tao, K.; Mogridge, J.; Kane, R. S. *Nat. Biotechnol.* **2006**, *24*, 582–586.
(21) Rai, P. R.; Saraph, A.; Ashton, R.; Poon, V.; Mogridge, J.; Kane, R. S. *Angew. Chem., Int. Ed.* **2007**, *46*, 2207–2209.
(22) Jugdutt, B. I. *Circulation* **2003**, *108*, 1395–1403.
(23) Myllyharju, J.; Kivirikko, K. I. *Ann. Med.* **2001**, *33*, 7–21.
(24) Cleutjens, J. P. M.; Blankesteijn, W. M.; Daemen, M. J. A. P.; Smits, J. F. M. *Cardiovasc. Res.* **1999**, *44*, 232–241.
(25) Rekhter, M. D. *Cardiovasc. Res.* **1999**, *41*, 376–384.
(26) Arroyo, L. H.; Lee, R. T. *Cardiovasc. Res.* **1999**, *41*, 369–375.
(27) Katsuda, S.; Kaji, T. *J. Atheroscler. Thromb.* **2003**, *10*, 267–274.
(28) Caravan, P.; Das, B.; Dumas, S.; Epstein, F. H.; Helm, P. A.; Jacques, V.; Koerner, S.; Kolodziej, A.; Shen, L.; Sun, W. C.; Zhang, Z. *Angew. Chem., Int. Ed.* **2007**, *46*, 8171–8173.
(29) Helm, P. A.; Caravan, P.; French, B. A.; Jacques, V.; Shen, L.; Xu, Y.; Beyers, R. J.; Roy, R. J.; Kramer, C. M.; Epstein, F. H. *Radiology* **2008**, *247*, 788–796.
(30) Santoro, S. A.; Cunningham, L. W. *J. Clin. Invest.* **1977**, *60*, 1054–1060.
(31) Cejas, M. A.; Chen, C.; Kinney, W. A.; Maryanoff, B. E. *Bioconjugate Chem.* **2007**, *18*, 1025–1027.
(32) Patti, J. M.; Boles, J. O.; Hook, M. *Biochemistry* **1993**, *32*, 11428–11435.
(33) Rich, R. L.; Deivanayagam, C. C.; Owens, R. T.; Carson, M.; Hook, A.; Moore, D.; Symersky, J.; Yang, V. W.; Narayana, S. V.; Hook, M. *J. Biol. Chem.* **1999**, *274*, 24906–24913.
(34) Zong, Y.; Xu, Y.; Liang, X.; Keene, D. R.; Hook, A.; Gurusiddappa, S.; Hook, M.; Narayana, S. V. *EMBO J.* **2005**, *24*, 4224–4236.
(35) Krahn, K. N.; Bouten, C. V.; van Tuijl, S.; van Zandvoort, M. A.; Merkx, M. *Anal. Biochem.* **2006**, *350*, 177–185.
(36) Boerboom, R. A.; Krahn, K. N.; Megens, R. T.; van Zandvoort, M. A.; Merkx, M.; Bouten, C. V. *J. Struct. Biol.* **2007**, *159*, 392–399.
(37) Megens, R. T.; Oude Egbrink, M. G.; Cleutjens, J. P.; Kuijpers, M. J.; Schiffers, P. H.; Merkx, M.; Slaaf, D. W.; van Zandvoort, M. A. *Mol. Imaging* **2007**, *6*, 247–260.
(38) Xu, Y.; Rivas, J. M.; Brown, E. L.; Liang, X.; Hook, M. *J. Infect. Dis.* **2004**, *189*, 2323–2333.
(39) Reulen, S. W. A.; Brusselaars, W. W. T.; Langereis, S.; Mulder, W. J. M.; Breurken, M.; Merkx, M. *Bioconjugate Chem.* **2007**, *18*, 590–596.
(40) Johnsson, M.; Hansson, P.; Edwards, K. *J. Phys. Chem. B* **2001**, *105*, 8420–8430.
(41) Ashok, B.; Arleth, L.; Hjelm, R. P.; Rubinstein, I.; Onyuksel, H. *J. Pharm. Sci.* **2004**, *93*, 2476–2487.
(42) Lukyanov, A. N.; Torchilin, V. P. *Adv. Drug Delivery Rev.* **2004**, *56*, 1273–1289.

fragments were ligated in the *Nde* I and *Sap* I sites of the vector pTXB1 (IMPACT system, New England Biolabs) to yield pTXB1-6His-CNA35. The Y175K mutation was introduced using the QuickChange site-directed mutagenesis kit (Stratagene) using pTXB1-6His-CNA35 plasmid as the template and the primers 5′-CGGGAACAAGTAGTGTTTTCTATAAAAAAACGGGAGATA-TGCTACC-3′ and 5′-GGTAGCCATATCTCCCGTTTTTTTAT-AGAAAACACTACTTGTTCCCG-3′ to yield plasmid pTXB1-6His-CNA35-Y175K. The correct open reading frames for all constructs were confirmed by DNA sequencing (BaseClear). Expression plasmids for wt-CNA35 (pTXB1-6His-CNA35) and CNA35-Y175K (pTXB1-6His-CNA35-Y175K) were transformed into *E. coli* BL21 (DE3) cells. All proteins were expressed as described previously.[39] The BugBuster (Novagen) isolated proteins were directly applied to a column of 3 mL of HisBind resin (Novagen) charged with $NiSO_4$. The column was washed with bind buffer (20 mM Tris, 0.5 M NaCl, 5 mM imidazole, pH 7.9) followed by wash buffer (20 mM Tris, 0.5 M NaCl, 15 mM imidazole, pH 7.9). The column was then quickly flushed with elution buffer (20 mM Tris, 0.5 M NaCl, 1 M imidazole, pH 7.9). The eluted proteins were directly applied to a 7 mL column of chitin resin (New England Biolabs), equilibrated with chitin binding buffer (20 mM sodium phosphate, 0.1 mM EDTA, 0.5 M NaCl, pH 8). The column was washed with chitin binding buffer after which the column was quickly flushed with cleavage buffer (20 mM sodium phosphate, 0.1 mM EDTA, 0.5 M NaCl, pH 6) containing 50 mM MESNA and incubated overnight at room temperature. Proteins were eluted in cleavage buffer and pooled. The concentrations of wt-CNA35−MESNA and CNA35-Y175K−MESNA were determined by UV−vis using $\varepsilon_{280nm} = 31\,400\ M^{-1}\ cm^{-1}$ and $\varepsilon_{280nm} = 29\,910\ M^{-1}\ cm^{-1}$, respectively.

Synthesis of Protein-Functionalized Micelles. A mixture of 97.5 mol % Cys−PEG−DSPE and 2.5 mol % rhodamine-DPPE in chloroform was placed in a vial. After chloroform evaporation the obtained lipid film was rehydrated in 0.1 M sodium phosphate pH 8.5 with 50 mM MPAA and 10 mM TCEP, vortexed for 2 min, followed by 5 min of sonication. CNA35 or CNA35-Y175K was added in varying amounts depending on the required protein load per micelle. The pH was adjusted to ∼6.5 with 1 M sodium phosphate pH 9.2. After overnight incubation at room temperature the protein micelles were analyzed using sodium dodecyl sulfate−polyacrylamide gel electrophoresis (SDS−PAGE) to check for complete conversion to the lipidated protein. Micelles were dialyzed overnight against HBS (10 mM HEPES, 135 mM NaCl, pH 7.4) using 10 kDa slide-A-lyzer cups (Pierce) to remove MPAA and TCEP and stored at 4 °C.

Synthesis of Protein-Functionalized Liposomes. Cysteine liposomes were prepared by lipid film hydration as reported previously.[39] A mixture of DSPC (37 μmol), Gd-DTPA-bis(stearylamide) (25 μmol), cholesterol (33 μmol), rhodamine-DPPE (0.34 μmol), PEG−DSPE (2.5 μmol), and Cys−PEG−DSPE (2.5 μmol) was dissolved in $CHCl_3$/MeOH 4:1 (v/v) and concentrated under reduced pressure at room temperature. The obtained lipid film was hydrated in HBS buffer (2 mL). This dispersion was extruded five times at 65 °C through 200 nm polycarbonate membrane filters. Phospholipid concentrations were determined by phosphate analysis according to Rouser et al.[43] The amount of lipids per liposome was calculated using a lipid surface area of 0.6 nm^2 [44] and assuming unilamellar liposomes. NCL of cysteine liposomes with CNA35-Y175K−MESNA was performed in the presence of 50 mM MPAA and 10 mM TCEP at several liposome-to-protein ratios for 24 h at 20 °C at a pH > 6. The coupling efficiency was monitored via SDS−PAGE analysis. The amount of lipidated CNA35-Y175K was calculated by scanning of the SDS−PAGE gel and integration of the bands of unreacted and reacted protein. The number of proteins per liposome was then obtained by dividing the concentration of lipidated CNA35-Y175K by the liposome concentration. The CNA35-Y175K liposomes were ultracentrifuged in a Kontron Centrikon T-2060 ultracentrifuge with a TFT 70.38 rotor for 1 h at 270 000*g* and 20 °C, after which the liposomal pellet was resuspended in HBS pH 7.4. Pellet and supernatant were analyzed using SDS−PAGE to confirm the separation between reacted and unreacted protein. CNA35-Y175K liposomes were stored at 4 °C.

Dynamic Light Scattering. The hydrodynamic diameter of the micelles was determined by dynamic light scattering using an ALV 5000/60×0 instrument using a laser of 632.8 nm and a measuring angle of 90° relative to the incident beam. The samples were diluted in HBS to a final lipid concentration of approximately 50 μM and measured at room temperature.

Cryogenic Transmission Electron Microscopy Analysis of CNA35 Micelles. CNA35 micelles with on average 2 and 20 proteins were diluted in HBS pH 7.4 containing 10 mM TCEP to a lipid concentration of 348 μM (1 mg/mL) and centrifuged for 5 min at 13 000 rpm. Small aliquots of the micelles were applied on the cryogenic transmission electron microscopy (cryo-TEM) grids within the environmental chamber (100% humidity) of the Vitrobot instrument (FEI) at room temperature. Excess liquid was removed with filter paper in the Vitrobot instrument, and the grids were subsequently shot into liquid ethane. The vitrified samples were stored under liquid nitrogen and analyzed at −170 °C using the TU/e CryoTitan microscope (FEI).

Collagen Binding Assays. The 96 well EIA/RIA microplates (Corning) were coated overnight at 4 °C with 7.0 μg of rat tail collagen type I in HBS per well. After overnight incubation, the plates were blocked with HBS containing 5% (w/v) skim milk powder (MHBS) for 1 h at room temperature. After washing the plates three times with HBS, the plates were incubated with micelles in MHBS for 3 h at room temperature. The fluorescence of the rhodamine-containing micelles was measured after eight wash steps with HBS at 620 nm in duplicate on a Thermo Fluoroskan Ascent FL plate reader using excitation of 578 nm.

Surface Plasmon Resonance. Sensorgrams were obtained on a Biacore T100 (GE Healthcare) using C1 chips functionalized with different collagens using standard EDC/NHS protocols. All binding experiments were performed at 25 °C using HBS as running buffer at a flow rate of 30 μL/min. Regeneration of the chips was performed with a 30 s injection of 2:3 mixture of 2-propanol/50 mM NaOH. Aspecific binding and buffer effects were taken into account by subtracting the simultaneous response from a reference surface containing no collagen, but functionalized with ethanolamine instead.

Imaging Collagen in Rat Kidney Tissues. Frozen sections of rat kidney tissue on Starfrost microscope slides were defrosted followed by a 10 min acetone fixation and subsequent three wash steps in HBS. Wt-CNA35 micelles, or CNA35-Y175K micelles (40 μM lipid, 10 μM protein), or plain micelles (40 μM lipid) were incubated together with rabbit anticollagen type IV antibody (5 μg/mL) in 3% bovine serum albumin (BSA) and HBS for 3 h at room temperature in the dark. After washing with HBS, donkey antirabbit IgG-FITC (20 μg/mL) and 0.2 μM DAPI in 3% BSA and HBS were incubated for 30 min in the dark. After washing with HBS the sections were mounted using FluorSafe (VWR) and covered with a glass coverslip. Images were obtained using an inverted Zeiss Axiovert 200 microscope coupled to an LSM 510 Meta (Carl Zeiss, Germany) laser scanning microscope with a 20× objective. Donkey antirabbit FITC and rhodamine containing micelles were excited using a argon laser (488 nm) and a helium−neon laser (543 nm), respectively. The two PMTs were defined as follows: 500−550 nm, FITC (PMT1) and 565−615 nm, rhodamine micelles (PMT2).

Results

CNA35 with a C-terminal thioester (CNA35−MESNA) was obtained after expression as an intein-fusion protein, followed by MESNA-induced cleavage between CNA35 and the intein domain. Since the high concentrations of thiophenol that are

(43) Rouser, G.; Fkeischer, S.; Yamamoto, A. *Lipids* **1970**, *5*, 494–496.
(44) Strijkers, G. J.; Mulder, W. J.; van Heeswijk, R. B.; Frederik, P. M.; Bomans, P.; Magusin, P. C.; Nicolay, K. *Magma* **2005**, *18*, 186–192.

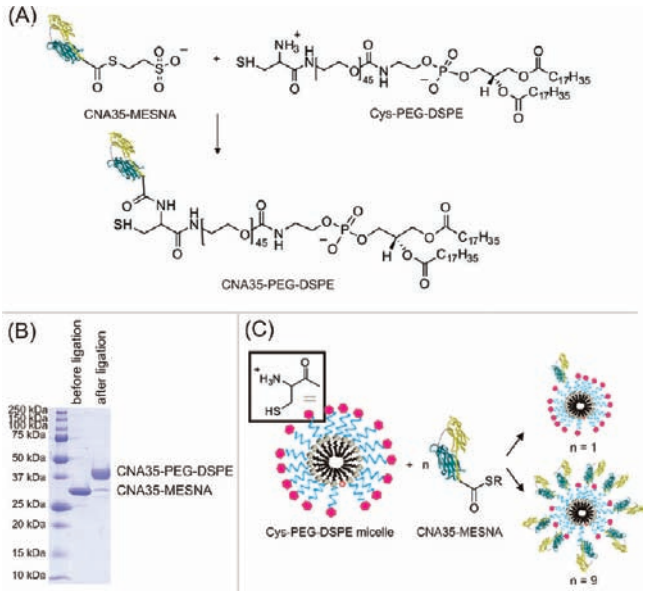

Figure 1. Preparation of multivalent CNA35 micelles. (A) Native chemical ligation of CNA35 with a C-terminal MESNA thioester to Cys−PEG−DSPE lipids resulting in a native peptide bond at the ligation site. (B) Representative SDS−PAGE gel showing the conversion of CNA35−MESNA to the lipidated form CNA35−PEG−DSPE. (C) Cys−PEG−DSPE and rhodamine-DPPE in a 40:1 ratio self-assemble into micelles in water. The average number of CNA35 proteins per micelle can be tuned by varying the CNA35 to lipid ratio in the NCL reaction.

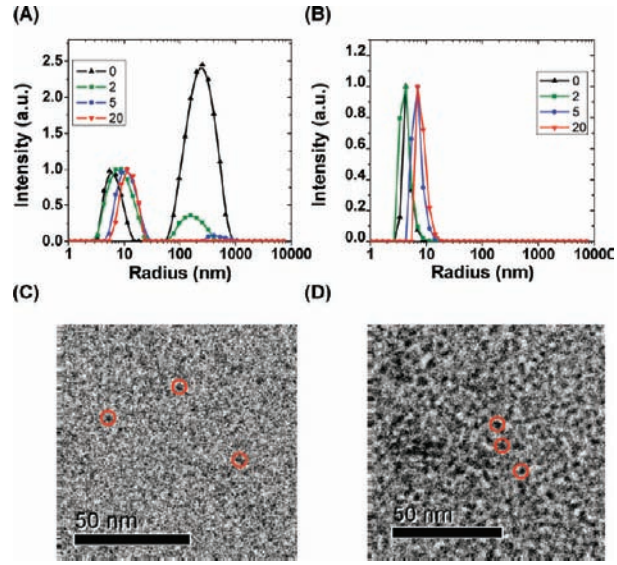

Figure 2. DLS and cryo-TEM analysis of multivalent CNA35 micelles. DLS analysis of CNA35 micelles with on average 0, 2, 5, and 20 proteins per micelle showing the intensity profile (A) and the volume profile (B). Cryo-TEM images of CNA35 micelles with on average 2 (C) and 20 (D) proteins per micelle with a lipid concentration of 348 μM (1 mg/mL). Magnification = 38 000. Scale bar = 50 nm.

typically used to catalyze NCL reactions might interfere with micelle formation, we tested whether MPAA could be used as a water-soluble alternative.[45] SDS−PAGE analysis indeed showed essentially complete conversion of CNA35−MESNA to CNA35−PEG2000−DSPE in the presence of MPAA (Figure 1, parts A and B), allowing one to calculate the average amount of proteins per micelle by simply dividing the protein concentration over the micelle concentration. The latter was calculated from the total amount of lipids and the previously reported aggregation number of 90 lipids per micelle.[41] By changing the lipid-to-protein ratios in the NCL reaction, micelles with an average protein content varying between 0 and 20 CNA35 proteins were obtained (Figure 1C).

Independent evidence for the formation of protein-functionalized micelles was obtained from dynamic light scattering (DLS) and cryo-TEM measurements (Figure 2). DLS showed a clear shift to higher diameter going from 13 nm for unfunctionalized micelles to 22 nm for a protein micelle with 20 proteins attached (Figure 2A). This increase in diameter is consistent with the addition of CNA35, which has a size of 6.5 nm × 4.1 nm × 2.3 nm.[34] Furthermore, functionalization with CNA35 also seemed to suppress the formation of a minor fraction of larger aggregates that was typically observed for Cys−PEG2000−DSPE at low protein−lipid ratios. Cryo-TEM analysis of CNA35 micelle preparations with 2 and 20 proteins per micelle confirmed the formation of well-defined micelles and the absence of significant amounts of larger aggregates. The dark spots shown in Figure 2, parts C and D, have a diameter of ~4 nm and correspond to the dense lipid core of the micelles. Cryo-TEM does not allow one to observe the more diffuse PEG/protein layer, which is consistent with previous studies that also showed poor contrast between PEG chains and the vitrified water matrix.[46]

To assess the effect of protein modification on micelle stability, the cmc of CNA35-functionalized micelles was determined by performing dilution experiments in the presence of the fluorescent dye 1,6-diphenyl-1,3,5-hexatriene (DPH). cmc's of ~5 μM were obtained for micelles with various amounts of CNA35 and nonfunctionalized Cys−PEG2000−DSPE micelles, which are similar to the cmc previously reported for PEG2000−DSPE (Supporting Information Figure S1).[40−42]

Incorporation of 2.5% rhodamine-DPPE in the CNA35 micelles allowed a direct assessment of the binding of these micelles to collagen-coated 96 well plates (Figure 3A). CNA35 micelles with on average 1, 5, and 21 proteins per micelle all bound to rat tail collagen type I, whereas no binding was observed for nonfunctionalized micelles or for CNA35 micelles in the absence of collagen. The same dependence on the lipid concentration was observed for all CNA35 micelles with half-maximal binding at 5−10 μM, suggesting that the binding behavior is determined by the cmc of these micelles and not the intrinsic affinity of these micelles for collagen. Interestingly, at saturating conditions more rhodamine fluorescence was observed for micelles with a low number of CNA35 proteins, which suggests that micelles with a high number of CNA35 proteins block multiple binding sites for CNA35 on collagen, resulting in the binding of less micelles per collagen.

Because the K_d for the monovalent interaction between CNA35 and collagen (~0.5 μM) is substantially lower than the cmc, both monovalent and multivalent interactions will be saturated at concentrations above the cmc. To resolve the importance of multivalency for the interaction between these protein micelles and collagen, the monovalent interaction between CNA35 and collagen was deliberately attenuated by replacement of a key residue in the collagen binding pocket, tyrosine 175 by a lysine. This Y175K

(45) Johnson, E. C.; Kent, S. B. *J. Am. Chem. Soc.* **2006**, *128*, 6640–6646.

(46) Johnsson, M.; Edwards, K. *Biophys. J.* **2003**, *85*, 3839–3847.

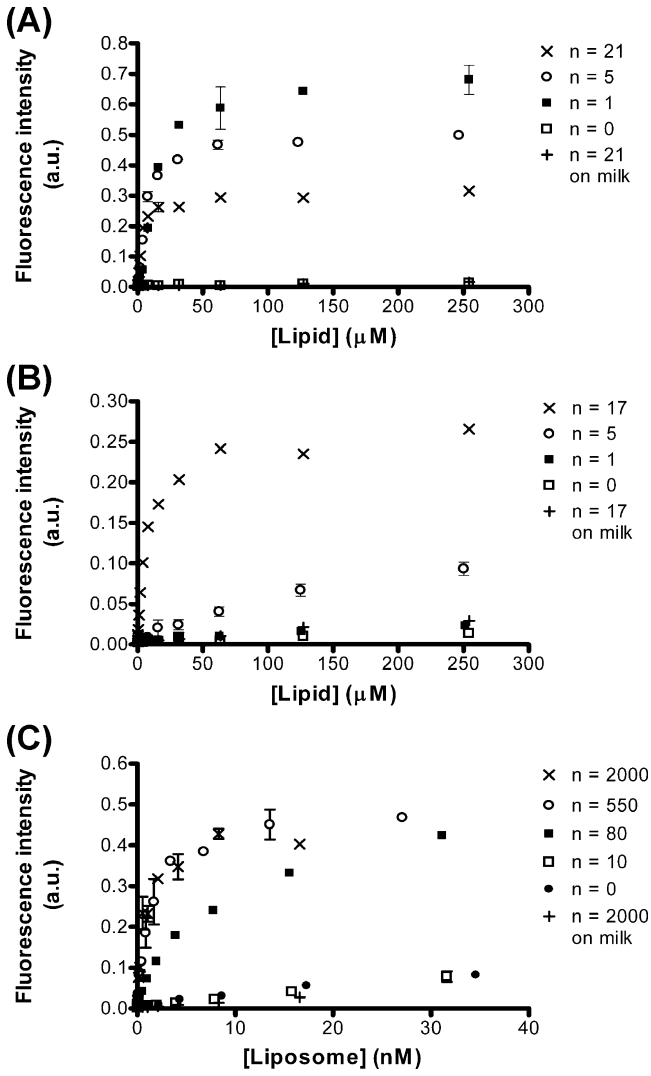

Figure 3. Binding of CNA35 micelles, CNA35-Y175K micelles, and CNA35-Y175K liposomes to rat tail collagen type I studied using solid-phase fluorescent binding assays. (A) Binding of CNA35 micelles with 0 (□), 1 (■), 5 (○), and 21 (×) proteins per micelle. A control experiment using CNA35 micelles ($n = 21$, +) incubated on milk powder is shown for comparison. (B) Binding of CNA35-Y175K micelles with 0 (□), 1 (■), 5 (○), and 17 (×) proteins per micelle. A control experiment using CNA35-Y175K micelles ($n = 17$, +) incubated on milk powder is shown for comparison. (C) Binding of CNA35-Y175K liposomes with 0 (●), 10 (□), 80 (■), 550 (○), and 2000 (×) proteins per micelle. A control experiment using CNA35-Y175K liposomes ($n = 2000$, +) incubated on milk powder is shown for comparison. Micelle and liposome binding was monitored by measuring the fluorescence of the rhodamine lipids at 620 nm using an excitation wavelength of 578 nm.

mutation was previously shown to decrease the collagen affinity by at least 900-fold and has thus been referred to as a "nonbinding" mutant.[47]

Remarkably, micelles functionalized with this nonbinding mutant did show collagen binding, but in this case the amount of binding and the apparent affinity were strongly dependent on the valency (Figure 3B). Micelles with on average one mutant protein showed no binding to rat tail collagen type I up to 300 μM lipid. Micelles with five copies of the CNA35-Y175K showed some binding, but the binding was not saturated at 300 μM. Saturated binding to a response level that is comparable to that of the wt-CNA35 micelles was observed only for the micelles with an average valency of 17 CNA35-Y175K proteins.

This impressive gain in binding affinity inspired us to apply the same strategy to CNA35-functionalized liposomes. Liposomes containing 2.5% Cys−PEG−DSPE were reacted with various amounts of CNA35-Y175K−MESNA. Upon removal of unreacted proteins using ultracentrifugation, the average number of proteins per 200 nm liposome could be calculated using the ligation efficiency determined via SDS−PAGE. Liposomes with high numbers of the nonbinding CNA35-Y175K protein ($n = 550$ and $n = 2000$) showed specific binding to rat tail collagen type I with dissociation constants in the low nanomolar range, similar to the 3 nM dissociation constant that was previously reported for liposomes containing wt-CNA35.[39] The collagen binding affinity was attenuated at a lower protein-to-liposome ratio of 80, whereas no binding was observed for liposomes with 10 proteins attached. These results show that "restoration" of the collagen affinity of the "nonbinding" CNA35-Y175K does not depend on the nature of the scaffold and demonstrates the potential of multivalent protein micelles (and liposomes) to enhance the affinity of very weak interactions for targets with multiple binding sites such as collagen.

A second striking observation from the micellar binding studies was that the fluorescent signal did not decrease even after extensive washing, suggesting that the stability of the collagen-bound micelles was enhanced compared to their stability in solution. Therefore, the binding of CNA35 micelles and collagen was studied in more detail using surface plasmon resonance (SPR), which allows monitoring of both the association and dissociation kinetics. Micelles with different amounts of wt-CNA35 (Figure 4A) or CNA35-Y175K (Figure 4B) were flowed over immobilized rat tail collagen type I for 10 min, followed by dissociation in the same buffer without micelles.

A robust increase in signal was observed for all wt-CNA35 micelles, whereas no signal was observed for nonfunctionalized micelles. Please note that SPR measures the increase in surface-bound mass, in contrast to the fluorescent assay described above which measured the number of micelles. If the SPR signal would be corrected for the substantial differences in mass between the different micelles, the same trend would be observed as seen in the fluorescence assays, showing binding of more micelles with a low CNA35 loading compared to micelles with a high number of CNA35 proteins. Micelles with on average one copy of CNA35-Y175K showed hardly any binding to rat tail collagen type I, but significant binding was observed for micelles with 5 and 17 proteins per micelle, confirming the trend observed in the fluorescence binding experiments. The association rate of the CNA35 micelles is similar to that of the protein itself, but a striking difference is observed in the dissociation behavior. Whereas CNA35 by itself readily dissociates from the collagen surface within 10 min, almost no dissociation of CNA35 micelles was observed in this time frame. Binding of CNA35 micelles even persisted up to 8 h of continuously flowing buffer over the collagen surface (Supporting Information Figure S2), showing that surface-bound CNA35 micelles are remarkably stable.

Since multivalent binding of the CNA35-Y175K micelles to collagen is expected to critically depend on the local density of CNA35 binding sites, we tested whether these micelles would be able to differentiate between different types of collagen. Figure 5 compares the collagen specificity of wt-CNA35 and CNA35-Y175K proteins with those of wt-CNA35 micelles and

(47) Symersky, J.; Patti, J. M.; Carson, M.; House-Pompeo, K.; Teale, M.; Moore, D.; Jin, L.; Schneider, A.; DeLucas, L. J.; Hook, M.; Narayana, S. V. *Nat. Struct. Biol.* **1997**, *4*, 833–838.

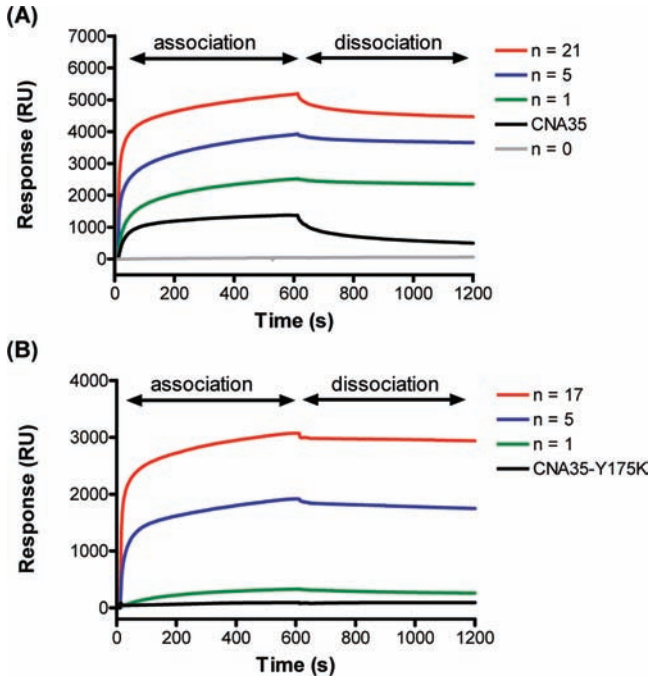

Figure 4. Binding of wt-CNA35 micelles and CNA35-Y175K micelles to rat tail collagen type I studied using surface plasmon resonance. (A) SPR analysis of CNA35 micelles binding to rat tail collagen type I. Micelles with on average 0, 1, 5, and 21 CNA35 proteins per micelle were injected at a lipid concentration of 40 μM in HBS on a C1 chip functionalized with rat tail collagen type I (1532 RU bound) for 10 min followed by a 10 min dissociation phase. For comparison wt-CNA35 was injected at a concentration of 0.5 μM in HBS on the same chip. (B) SPR analysis of CNA35-Y175K micelles binding to rat tail collagen type I. Protein micelles with on average 1, 5, and 17 proteins per micelle were injected at a lipid concentration of 40 μM in HBS on a C1 chip functionalized with rat tail collagen type I (1532 RU bound) for 10 min followed by a 10 min dissociation phase. For comparison CNA35-Y175K was injected at a concentration of 4 μM in HBS on the same chip.

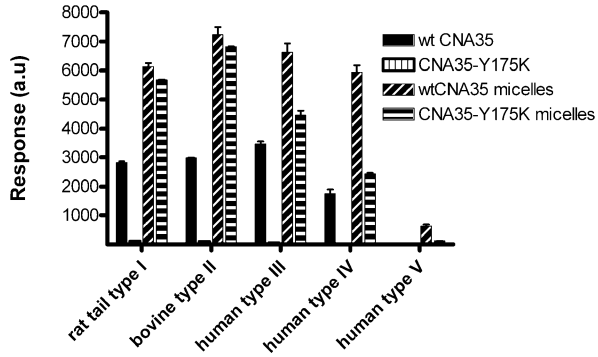

Figure 5. SPR analysis of collagen specificity for wt-CNA35, CNA35-Y175K, wt-CNA35 micelles, and CNA35-Y175K micelles. Protein micelles with on average 20 proteins per micelle were injected at a lipid concentration of 40 μM (protein concentration = 10 μM) in HBS on C1 chips functionalized with collagen type I (1357 RU bound), collagen type II (1486 RU bound), collagen type III (1685 RU bound), collagen type IV (1512 RU bound), and collagen type V (2029 RU bound) for 10 min. Wt-CNA35 and CNA35-Y175K were injected at a protein concentration of 10 μM in HBS for 10 min. The graph shows the binding response obtained after 10 min of association.

CNA35-Y175K micelles, each of which contained 20 proteins per micelle. All binding experiments were performed at the same protein concentration (10 μM), which corresponds to a lipid concentration of 40 μM for the micelles. First, these experiments showed that the remarkable increase in collagen affinity for multivalent CNA35-Y175K micelles was observed for all collagen types that also bound wt-CNA35. Although subtle differences in the binding level were observed between micelles with wt-CNA35 and CNA35-Y175K, the overall specificity of the CNA35-Y175K micelles mirrored that of wt-CNA35 and wt-CNA35 micelles. Apparently, collagen types I−IV all provide a sufficient density of binding sites to sustain multivalent binding, despite the fact that type IV collagen forms network-like collagen architectures, whereas types I−III form fibers.[48] Neither CNA35 nor CNA35 micelles bound to collagen type V, a type of collagen that is normally found associated with other collagens. Collagen type V often forms heterofibrils in which collagen type V is located in the core of collagen type I fibrils.[23]

To assess how the remarkable collagen binding properties of the micelles with the nonbinding CNA35 variant translate to the imaging of collagen in native tissues, we tested their performance on rat renal tissue. The kidneys contain approximately one million nephrons, each consisting of a glomerulus connected to a tubular system. The most abundant protein in the basement membranes of both the glomerulus and the tubular system is collagen type IV, whereas small amounts of collagen types I and III are also present in the interstitium.[49] Kidney tissue sections were incubated with rhodamine-labeled micelles containing either 20 copies of wt-CNA35, 20 copies of CNA35-Y175K, or nonfunctionalized micelles. Specific staining of collagen architectures was observed in the tubuli with both wt-CNA35 micelles (Figure 6A) and CNA35-Y175K micelles (Figure 6D), whereas no staining was observed using the nonfunctionalized micelles (Figure 6G). To confirm that the micelles were specifically targeting collagen, a costaining experiment was done using a collagen type IV specific antibody (green channel). Significant overlap was observed between the protein micelles and the collagen type IV specific antibody, confirming the collagen specificity of the micellar targeting. (Figure 6, parts C and F). The incomplete overlap between both probes is probably due to a more limited tissue penetration of the micelles compared to the antibody, although we can also not rule out subtle differences in binding specificity. Specific staining of collagen was also observed in the basal membrane of the glomeruli using both wt-CNA35 micelles (Figure 7A) and CNA35-Y175K micelles (Figure 7D), and again no binding was observed using nonfunctionalized micelles (Figure 7G). However, in this case a significant difference was observed between the wt-CNA35 micelles and CNA35-Y175K micelles. CNA35-Y175K only stained collagen structures in the basal membrane of the glomerulus, whereas wt-CNA35 micelles and collagen type IV specific antibodies also stained collagens at the inside of the glomerulus. Despite these differences, these ex vivo collagen imaging experiments nonetheless clearly show that the micelles with the so-called nonbinding CNA35 variant are able to bind to mature, unprocessed, organized collagens in native tissue.

Discussion

The approach presented here takes advantage of the chemoselectivity and efficiency of NCL to prepare relatively well-defined and stable protein-functionalized micelles with a tunable valency. A key advantage of this method is that proteins are

(48) Gelse, K.; Poschl, E.; Aigner, T. *Adv. Drug Delivery Rev.* **2003**, *55*, 1531–1546.
(49) Alexakis, C.; Maxwell, P.; Bou-Gharios, G. *Nephron Exp. Nephrol.* **2006**, *102*, E71–E75.

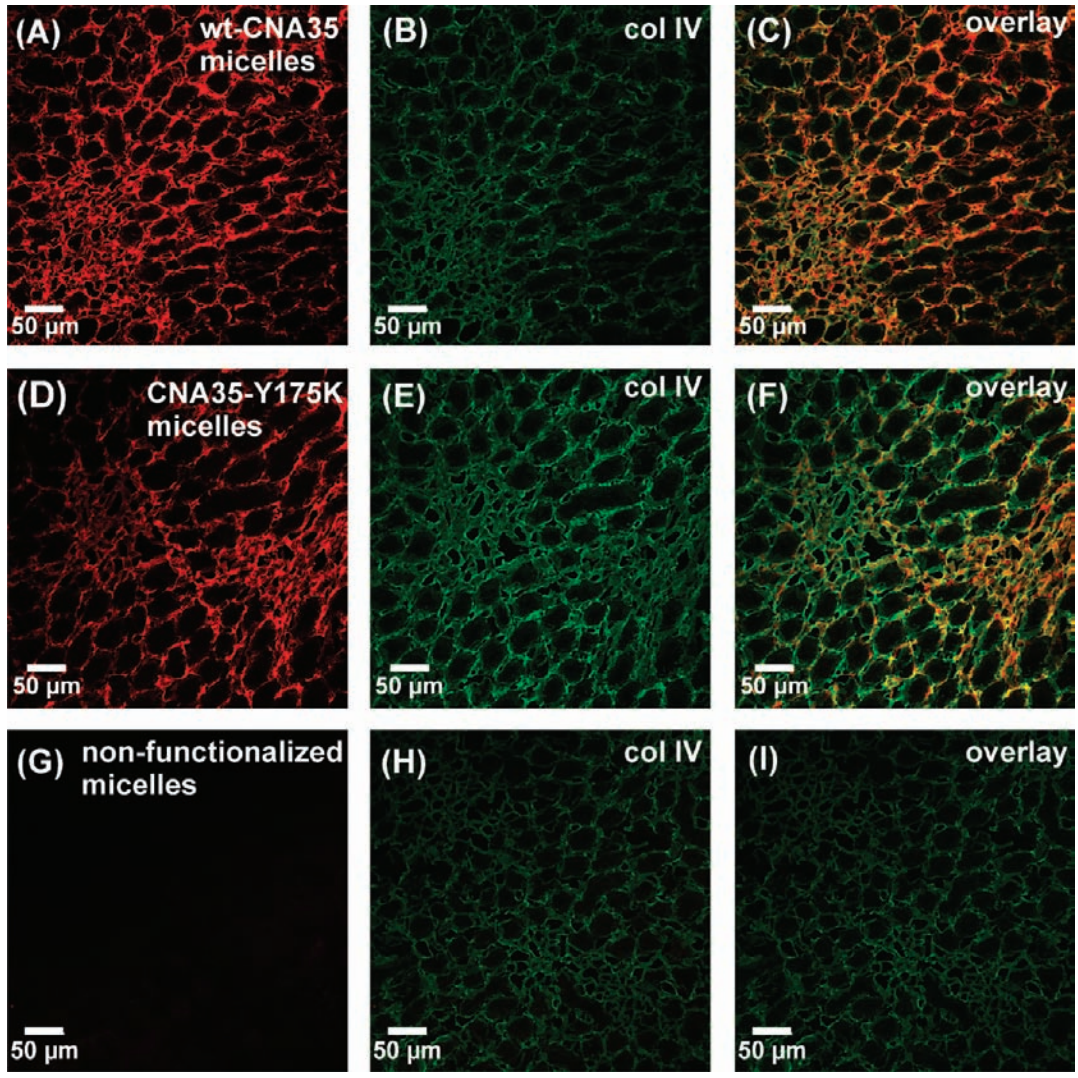

Figure 6. Confocal laser scanning microscopy images of tubular structures from rat kidney tissue incubated with wt-CNA35 micelles (A−C), or CNA35-Y175K micelles (D−F), or plain micelles (G−I) in the presence of rabbit anticollagen type IV antibody and, additionally, with donkey antirabbit IgG-FITC. The red channel shows the rhodamine-labeled micelles, while the green channel shows binding of anticollagen type IV antibody.

coupled specifically via their C-terminus. Current preparation methods for protein micelles are based on conjugation to amine functionalities on proteins, either directly by reaction to amine-reactive phospholipids such as *p*-nitrophenylcarbonyl−PEG−DOPE, or after SATA modification of the amines to thiols, followed by reaction with maleimide-functionalized PEG−DSPE.[1,50,51] These classical bioconjugation strategies suffer from a lack of control, however, yielding heterogeneous conjugates and in some instances a substantial decrease in binding activity. The strategy described here is generally applicable, not only for the preparation of protein and peptide micelles, but also for other lipid-based nanoparticles such as lipid-coated quantum dots and iron oxide nanoparticles.[2,52]

Understanding the multivalent interactions between micelles and complex biomolecular targets such as collagen is critical to allow efficient use of targeted micelles in drug delivery and molecular imaging. Surprisingly little is known about the importance of multivalent interactions on the affinity of micellar targeting and the influence of such interactions on micelle stability. Multivalency has been reported to affect cellular uptake of RGD-functionalized micelles, but the importance of multivalency for the interaction between these micelles and integrin architectures on the cell surface was not directly determined.[9] Polymeric micelles similar to the ones reported here have previously been functionalized with antibodies, but the effect of antibody loading has not been addressed, either in vivo or in vitro.[1,7,8] As far as we know this study therefore presents the first convincing demonstration that multivalent presentation on a micellar scaffold can enhance the affinity of a protein ligand many orders of magnitude, from apparently nonbinding to an affinity that is similar to that of the native collagen binding protein. A similar phenomenon was observed using liposomes as a multivalent scaffold, suggesting that it is the surface density of proteins that determines the multivalent enhancement of

(50) Mulder, W. J.; Strijkers, G. J.; Griffioen, A. W.; van Bloois, L.; Molema, G.; Storm, G.; Koning, G. A.; Nicolay, K. *Bioconjugate Chem.* **2004**, *15*, 799–806.
(51) van Tilborg, G. A.; Mulder, W. J.; Deckers, N.; Storm, G.; Reutelingsperger, C. P.; Strijkers, G. J.; Nicolay, K. *Bioconjugate Chem.* **2006**, *17*, 741–749.
(52) Mulder, W. J.; Koole, R.; Brandwijk, R. J.; Storm, G.; Chin, P. T.; Strijkers, G. J.; de Mello Donega, C.; Nicolay, K.; Griffioen, A. W. *Nano Lett.* **2006**, *6*, 1–6.

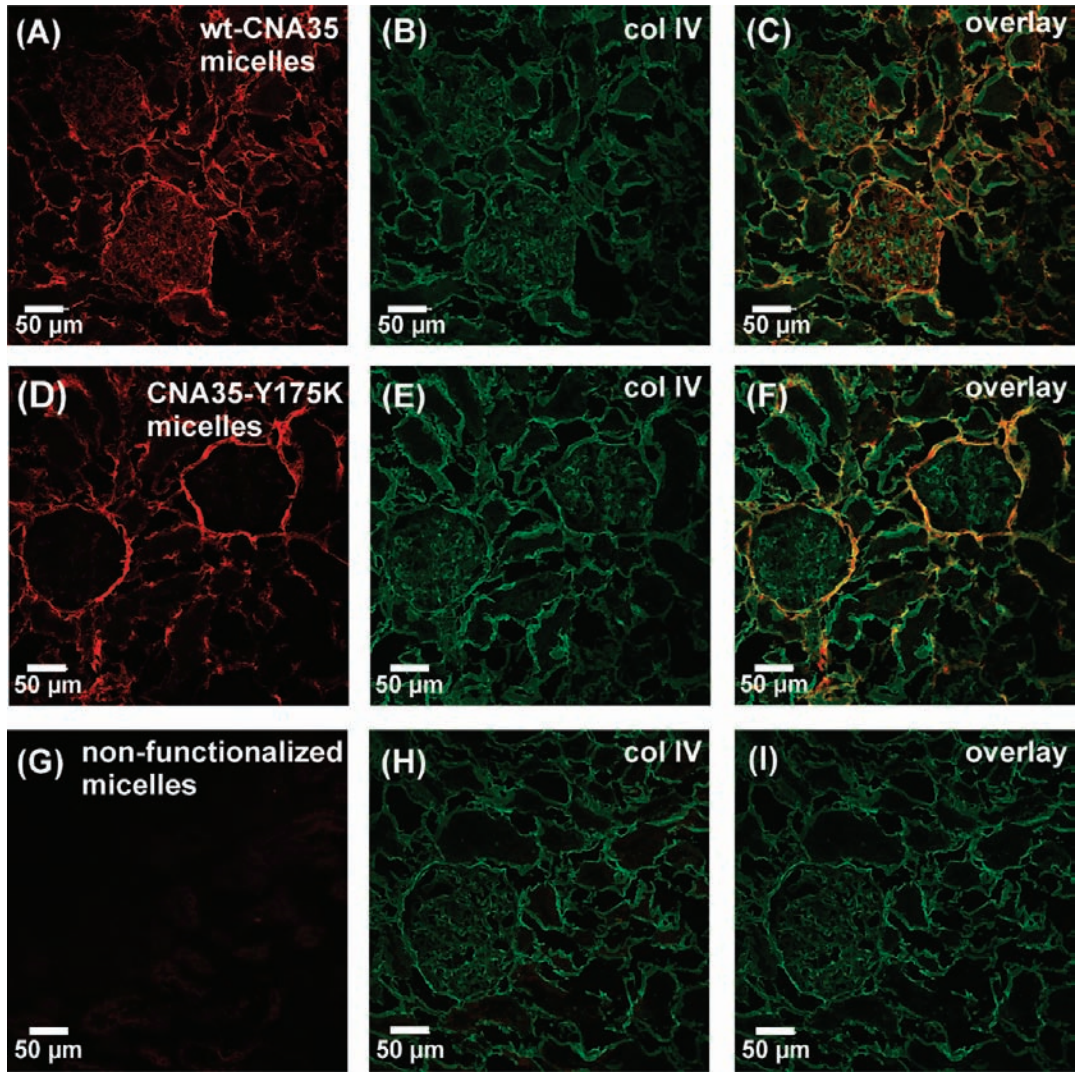

Figure 7. Confocal laser scanning microscopy images of glomerular structures from rat kidney tissue incubated with wt-CNA35 micelles (A−C), or CNA35-Y175K micelles (D−F), or plain micelles (G−I) in the presence of rabbit anticollagen type IV antibody and, additionally, with donkey antirabbit IgG-FITC. The red channel shows the rhodamine-labeled micelles, while the green channel shows binding of anticollagen type IV antibody.

collagen affinity. Indeed, a quick comparison shows that micelles and liposomes that display a high collagen affinity have similar protein densities of ~10 000 proteins/μm^2. Attenuation of collagen affinity is observed for liposomes carrying 80 proteins/liposome (640 proteins/μm^2) and micelles carrying on average five copies of CNA35-Y175K (3300 protein/μm^2), whereas no binding is observed with 10 proteins attached per liposome (80 proteins/μm^2). Care should thus be taken when interpreting the results from experiments using "nonbinding" variants of targeting ligands, at least when displayed on a multivalent scaffold and targeting a multivalent receptor.

The second important finding from this study is that micelles bound to a surface via multivalent interactions appear to be significantly more stable than micelles in solution. The SPR experimental setup in which buffer was continuously flowed over the collagen-bound CNA35 micelles can be regarded as an appropriate model for target-bound micelles in vivo. This remarkable effect may at least partially explain why micelles, despite their dynamic nature and relative instability, have been used quite successfully in targeted drug delivery and molecular imaging. This effect of multivalency on micelle stability is not without precedent. Studying the interaction between lactose-functionalized micelles and a surface with a high density of carbohydrate binding RCA-I lectines, Jule and co-workers also reported a dramatic decrease in micelle dissociation rate, but only at high ligand densities.[12,14] In contrast, a similar effect was not observed in a more recent study using multivalent α-D-mannopyranosides-functionalized micelles and concavalin A surfaces.[13] Significantly smaller micelles with lower ligand densities were used in the latter study, however, suggesting that proper matching between the average distance between ligands on the micelle and multivalent receptor sites may be essential for this type of stabilization.

The fact that CNA35 micelles do not readily dissociate once bound to collagen is an attractive feature from the perspective of the molecular imaging of collagen in vivo. Pegylated phospholipids functionalized with targeting ligands can simply be mixed with amphiphiles carrying different spectral probes to allow simultaneous detection using a variety of imaging modalities such as fluorescence, MRI and single-photon emission computed tomography (SPECT). The present results also corroborate recent findings from our group showing that the affinity of phage-display-derived collagen binding peptides can be significantly enhanced by multivalent

display on a dendritic scaffold.[53] Potentially even more interesting than the effect on binding affinity is the possibility to employ multiple weak interactions to distinguish between similar biomolecular architectures based on the density of ligand binding sites.[54,55] One reason that we did not observe clear differences in collagen specificity between CNA35-Y175K micelles and wt-CNA35 micelles may be that their dynamic nature allows micelles to adjust to different binding site architectures. At present, very little is known about dynamics of proteins within the micelle or the kinetics of protein exchange between micelles. Work addressing the latter question using micelles functionalized with donor and acceptor fluorescent proteins is in progress and will be reported elsewhere. Interestingly, we did observe a difference in specificity using both types of micelles when imaging collagen type IV in rat kidney tissue, with the CNA35-Y175K micelles apparently detecting only a subset of the type IV collagen architectures.[56] Given the complexity of natural collagen it will be difficult to establish whether this apparent specificity is really due to a different binding site density. Instead, these questions are probably better first addressed using model surfaces based on synthetic collagen peptides that allow a better control of binding site architecture.

Acknowledgment. The authors thank Nico A. J. M. Sommerdijk for support on the cryo-TEM measurements, Monica Breurken for supplying the plasmid pTXB1-6His-CNA35 and the protein CNA35-OG488, Marcel Rooijackers for cloning the CNA35-Y175K variant, Erik Sanders for cysteine liposome preparation, and Roy LeClercq and Sander Langereis (Philips Research, Eindhoven, The Netherlands) for performing the DLS measurements. This work was supported by an NWO VIDI Grant 700.56.428 to M.M. and the BSIK program entitled Molecular Imaging of Ischemic Heart Disease (project no. BSIK03033).

Supporting Information Available: Experimental details including the cmc determination of the protein micelles and Biacore analysis of the dissociation kinetics of CNA35 micelles and CNA35. This material is available free of charge via the Internet at http://pubs.acs.org.

JA807723P

(53) Helms, B.; Reulen, S. W. A.; Nijhuis, S.; de Graaf-Heuvelmans, P. T. H. M.; Merkx, M.; Meijer, E. W. *J. Am. Chem. Soc.* Submitted for publication, 2009.
(54) Kiessling, L. L.; Gestwicki, J. E.; Strong, L. E. *Angew. Chem., Int. Ed.* **2006**, *45*, 2348–2368.
(55) Carlson, C. B.; Mowery, P.; Owen, R. M.; Dykhuizen, E. C.; Kiessling, L. L. *ACS Chem. Biol.* **2007**, *2*, 119–127.
(56) Miner, J. H. *Kidney Int.* **1999**, *56*, 2016–2024.